Global gyrokinetic investigation of Alfvén instabilities and turbulence in tokamaks

A. Biancalani[1], A. Bottino[1], A. Di Siena[2], Ö. Gürcan[3], F. Jenko[1], P. Lauber[1], A. Mishchenko[4], P. Morel[3], I. Novikau[5], F. Vannini[1], L. Villard[6], and A. Zocco[4]

[1]Max-Planck Institute for Plasma Physics, 85748 Garching, Germany;
[2]University of Texas at Austin, Austin, TX-78712, USA
[3]LPP, CNRS, École polytechnique, UPMC, Univ. Paris-Sud, 91128 Palaiseau, France
[4]Max-Planck Institute for Plasma Physics, D-17491 Greifswald, Germany
[5]Princeton Plasma Physics Laboratory, NJ-08540 Princeton, USA
[6]EPFL-SPC, CH-1015 Lausanne, Switzerland

Contacts of main author: biancalani@ipp.mpg.de

1. Introduction and motivation

- Alfvén Modes (AM) are oscillations of perpendicular magnetic field, [Appert-82, Chen-16], important for interaction with energetic particle (EP) population.
- EP population is consequently redistributed in phase space if wave-particle nonlinearity is effective
  → plasma heating is less effective and EP losses occur.
- Zonal Structures (ZS) like zero-frequency zonal flows (ZF) and geodesic acoustic modes (GAM) are often observed in the presence of turbulence [Winsor-68, Hasegawa-79]
- A kinetic treatment is known to be necessary due to:

  1) the low frequencies ($> \sim \omega_{ti}$), where resonances with bulk ions substantially modify the MHD predictions

  2) the wave-particle interaction responsible for the EP drive and Landau damping.

  3) kinetic modific. to wave-wave inter. (expecially for $k_\perp \rho_i \sim 1$)
- Dynamics slower than gyrofrequencies → GK ordering valid.
- EP redistribution depends on AM saturation levels.
- Several saturation mechanisms should be investigated theoretically and compared with experiments:

↪ wave-particle trapping
↪ EP radial redistribution
↪ resonance overlapping
↪ mode-mode coupling

- Toroidicity induced Alfvén Eigenmodes (TAE) observed in Ohmically heated AUG plasmas [Maraschek-97]
- Excitation of AM without EP → evidence of strong coupling of AM and short wavelength drift Alfvén turbulence.

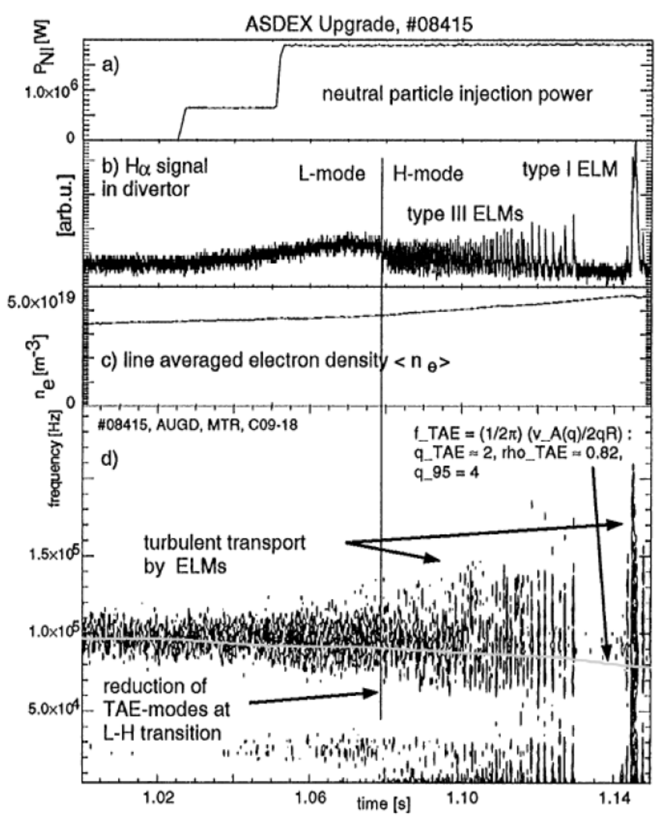

Fig. 1 *Alfvén modes in Ohmically heated plasmas [Maraschek-97]*

- Interaction of EPs and turbulence has been observed
  ↪ in experiments [Tardini-07, Heidbrink-09, Romanelli-10, Bock-17]
  ↪ investigated by means of analytical theory [White-89, Chen-16, Zonca-15, Qiu-16]
  ↪ investigated by means of flux-tube numerical simulations [Angioni-09, Bass-10, Zhang-10, Citrin-13, Garcia-15, DiSiena-19, DiSiena-21].

2. Model and equilibrium

- ORB5 is a multispieces ele-magn. GK code [Jolliet-07, Lanti-20].
- ORB5 is global (i.e. it resolves modes with structure comparable with the minor radius → appropriate for studying low-n AMs
- A Krook operator is used as a source for the thermal species. It acts by restoring the initial thermal plasma profiles.
- Magnetic equilibrium with circular concentric flux surfaces and reversed shear [Biancalani-20].
- Large aspect ratio and gradients peaked at mid-radius for simplicity.
- $\rho^* = \rho_s/a = 2/350$, $\beta = 8\pi n(T_i + T_e)/B^2 = 1 \cdot 10^{-3}$.

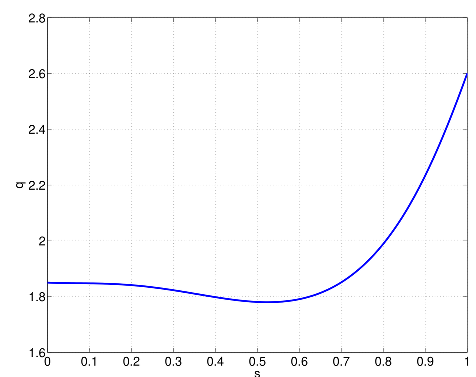

Fig. 2. *Reversed shear safety factor profile.*

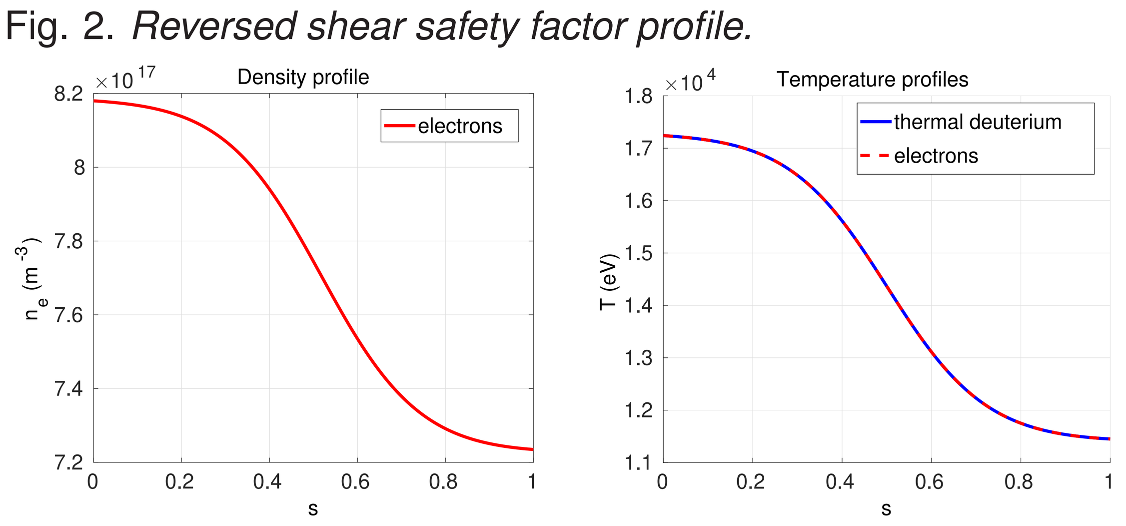

Fig. 3. *Density profile (left) and temperature profile (right).*

3. Turbulence and AM characterisation

Turbulence

- Ion-temperature-grdient (ITG) modes
- Most unstable mode at $n = 30$, with growth rate:

  $\gamma_{ITG,EM} = 4.25 \cdot 10^{-4}\,\Omega_i$
- No direct effect of the EPs on the ITG dynamics in this regime

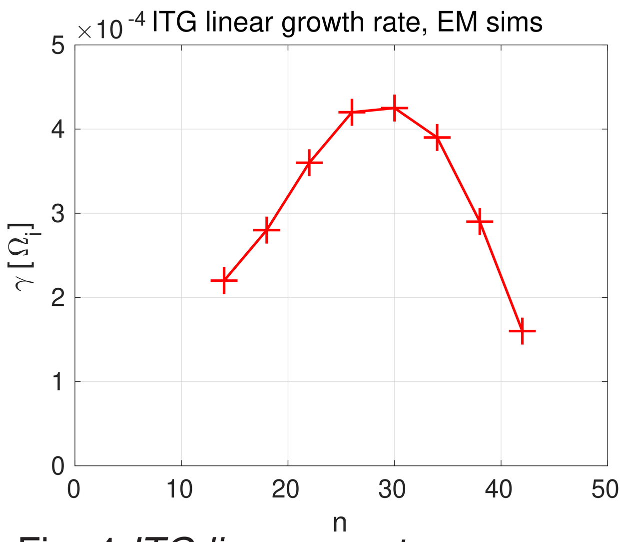

Fig. 4 *ITG linear spectrum*

Ratios of ion over electron heat fluxes: $\kappa_{ITG,i} = \langle\Gamma_i\rangle/\langle\Gamma_e\rangle = 2.7$, $\kappa_{ITG,EP} = \langle\Gamma_{EP}\rangle/\langle\Gamma_e\rangle = 0.14$.

Alfvén modes

- Maxwellian EP population with $\langle n_{EP}\rangle/\langle n_e\rangle = 0.01$
- Most unstable mode at $n = 5$, with growth rate:

  $\gamma_{AM} = 7 \cdot 10^{-4}\,\Omega_i$
- Beta induced Alfvén Eigenmode (BAE) identified, with $n = 5$, $m = 9$, peaked at $s = 0.39$ ($q = 1.8$ rational surface).

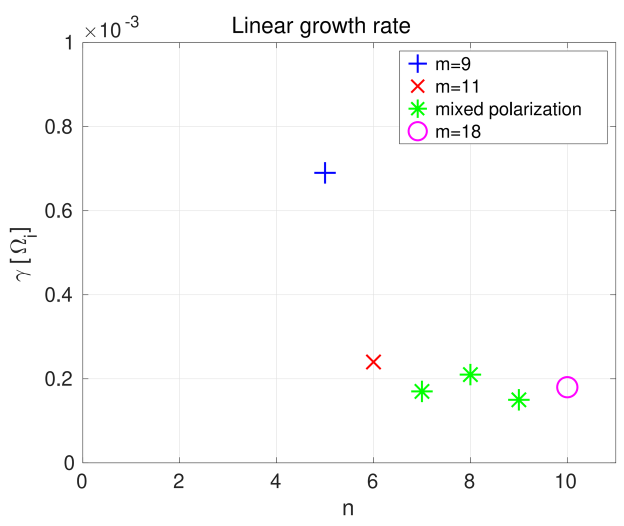

Fig. 5 *AM linear spectrum*

Ratios of ion over electron heat fluxes: $\kappa_{AM,i} = \langle\Gamma_i\rangle/\langle\Gamma_e\rangle = 0.7$, $\kappa_{AM,EP} = \langle\Gamma_{EP}\rangle/\langle\Gamma_e\rangle = 2.4$.

4. Turbulence with AMs: fields

- Fully NL electromagnetic simulation: WP-NL + WW-NL (all species follow perturbed orbits) [Biancalani-21]
- Noise initialized at t=0
- Toroidal filter allows $0 \leq n \leq 40$
- EP switched on at $t = 4.9 \cdot 10^4\,\Omega_i^{-1}$ Krook operator, conserving zonal fields, applied to thermal species: → source restoring thermal profiles, no sources for EPs

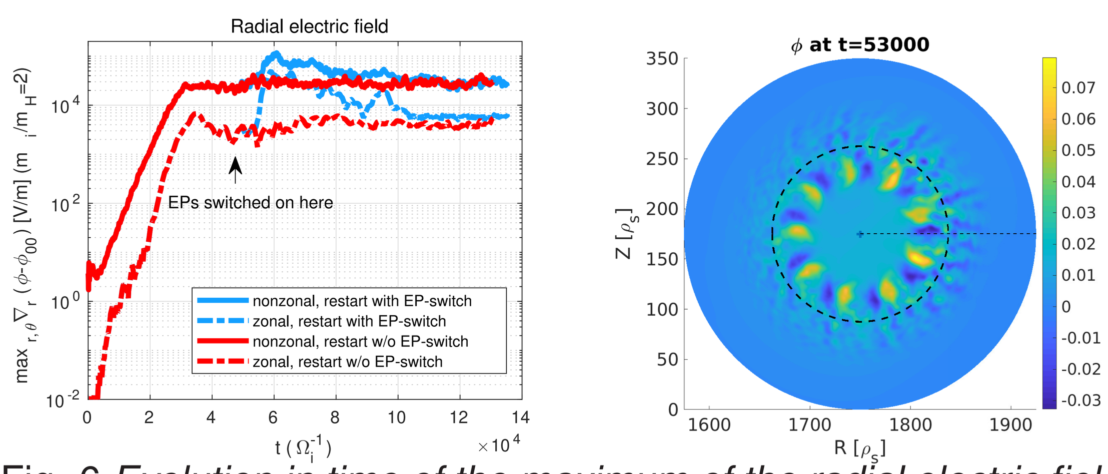

Fig. 6 *Evolution in time of the maximum of the radial electric field in the poloidal plane (left), and snapshot of the scalar potential after the EPs are switched on [Biancalani-21].*

- Turbulence and ZF forming and saturating in the first phase (before EP switch)
- BAE growing on top of turbulence after EP switch and saturating due to EP redistribution
- ZF also growing to higher levels due to forced-driven excitation by BAE [Todo-10,Qiu-16]

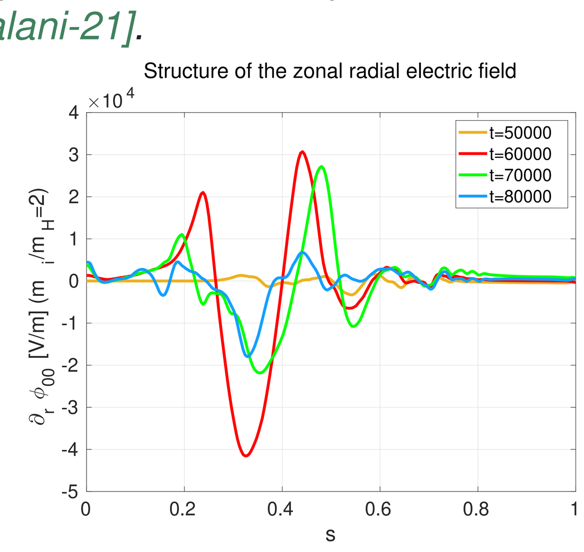

Fig. 7 *Radial structure of the ZF*

5. Turbulence with AMs: heat transport

- Strong heat flux after the EP switch (especially carried by EPs)
- Electron heat flux dominant over thermal ion heat flux → signature of AM activity [Biancalani-21]

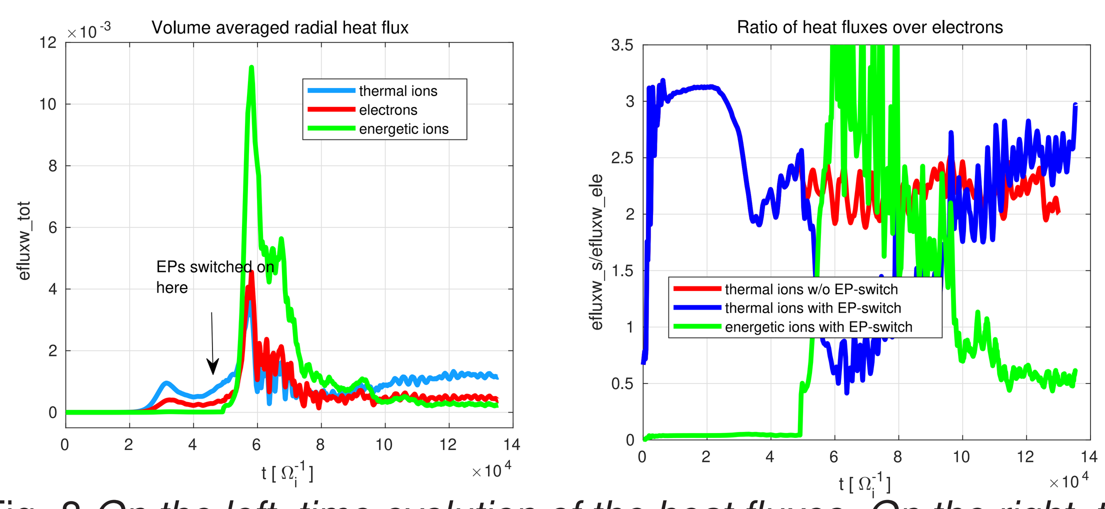

Fig. 8 *On the left, time evolution of the heat fluxes. On the right, the ratio of the heat fluxes divided by the heat flux of the electrons.*

6. Monotonic safety factor

- Simulations repeated with monotonic safety factor profile
- Rational surface of $q = 1.8$ located at mid-radius, $s = 0.5$
- BAE now co-localized with ITG turbulence
- Same saturation levels of ITG and BAE as in reversed-shear case
- ZF forced-driven by BAE now localized at mid-radius
- ZF shearing also higher for this case

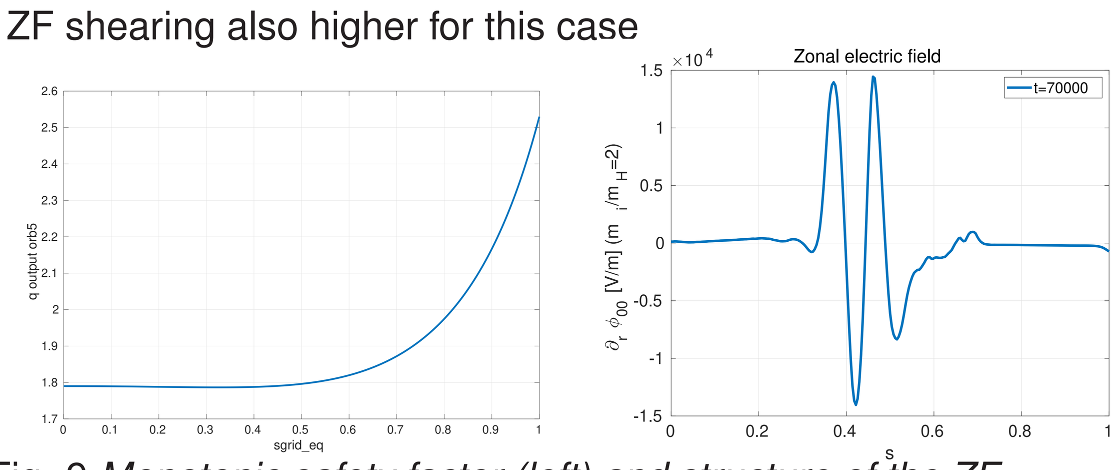

Fig. 9 *Monotonic safety factor (left) and structure of the ZF forced-driven by the BAE (right)*

- Heat flux levels similar to reversed-shear case
- Heat flux of electrons confirmed dominant over thermal ions after EP switch
  → this does not depend on the sign of the shear
- Stronger oscillations of the heat flux → GAM ?

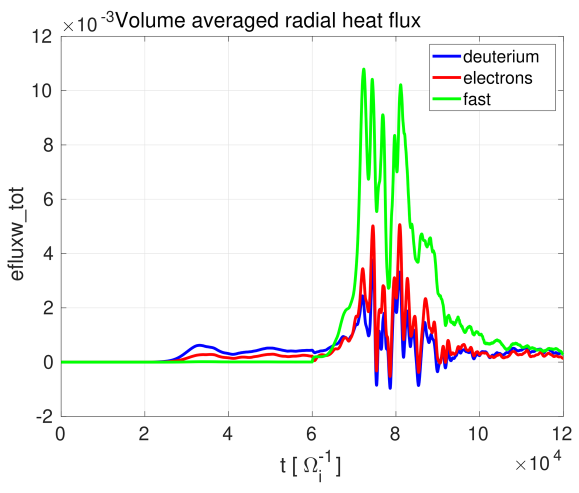

Fig. 10 *Heat flux for monotonic q*

7. Conclusions and outlook

- ORB5 capable of investigating selfconsistently global modes (like AM, and zonal structures) and turbulence and EPs.
- Global nonlinear simulations performed, with electrons treated fully (drift-)kinetically.
- AM driven unstable by EP on top of a turbulent plasma, saturate due to wave-particle + wave-wave coupling
- Zonal structures driven by ITG in the first phase, then by AM in the second phase
- Saturation levels and heat fluxes found not to depend on shear sign
- Study of the role of the zonal flow in progress
- Extension to more experimentally relevant cases in progress [Mishchenko-21]

Acknowledgements

This work has been carried out within the framework of the EUROfusion Consortium and has received funding from the Euratom research and training programme 2014-2018 and 2019-2020 under grant agreement No 633053, within the framework of the "MET" European Enabling Research Project. The views and opinions expressed herein do not necessarily reflect those of the European Commission. Discussions with F. Zonca, E. Poli, S. Brunner, B. McMillan, Z. Qiu, and T. Hayward-Schneider are gratefully acknowledged. Simulations were performed on the Marconi supercomputer within the framework of the ORBFAST and OrbZONE projects.

References

- Angioni C., et al., 2009 *Nucl. Fusion* **49**, 055013
- Appert K., et al. 1982 *Plasma Phys* **24**, 1147
- Bass E. M., Waltz, R. E., 2010 *Phys. Plasmas* **17** 11, 112319
- Biancalani A., et al., 2020 *J. Plasma Phys* **86**, 825860301
- Biancalani A., et al., 2021 *Plasma Phys. Control. Fusion* in press
- Bock A., et al., 2017 *Nucl. Fusion* **57** 126041
- Chen L. and Zonca F., 2012 *Phys. Rev. Lett.* **109**, 145002
- Chen L. and Zonca F., 2016 *Rev. Mod. Phys.* **88**, 015008
- Citrin J., et al., 2013 *Phys. Rev. Lett.* **111**, 155001
- Di Siena A., et al., 2019 *Nucl. Fusion*, **59**, 124001
- Di Siena A., et al., 2021 *IAEA FEC*, TH/4
- Garcia J., et al., 2015 *Nucl. Fusion* **55** 053007
- Hasegawa A., et al., 1979 *Phys. Fluids* **22**, 2122
- Heidbrink W. W., et al., 2009 *Phys. Rev. Lett.* **103**, 175001
- Holland C., et al., 2012 *Nucl. Fusion* **52**, 114007
- Jolliet S., et al., 2007 *Comput. Phys. Commun.* **177**, 409
- Maraschek M., et al., 1997 *Phys. Rev. Lett.* **79**, 4186
- Romanelli M., et al., 2010 *Pl. Phys. Control. Fusion* **52**, 045007
- Qiu Z., Chen L. and Zonca F., 2016 *Nucl. Fusion* **56**, 106013
- Tardini G., et al., 2007 *Nucl. Fusion* **47**, 280
- Todo Y., et al., 2010 *Nucl. Fusion* **50** 084016
- White R., et al., 1989 *Phys. Fluids B* **1**, 980
- Winsor N., et al., 1968 *Phys. Fluids* **11**, 2448
- Zhang W., et al., 2010 *Phys. Plasmas* **17**, 055902